

Use of FTIR Microscopic Imaging to Locate and Identify Contaminants on Electronic Components

Author

Robert Heintz

Industry/Application

Failure analysis, identification of contaminants, electronic components, FTIR imaging

Product Used

Thermo Scientific™ Nicolet™ iN10 MX Infrared Microscope

Goal

Demonstrate how FTIR microscopy and imaging can be used to locate and identify multiple contaminants on samples

Key Analytes

Oil, ester additives, cellulose, protein, plastic

Key Benefits

FTIR microscopy can be used to non-destructively identify unknown foreign materials on a device while leaving it undisturbed and intact. Imaging adds the ability readily locate and analyzing multiple contaminants while also providing a view of the distribution across the sample.

Introduction

Contamination analysis involves the identification of foreign material on or in a product. Contaminants are not only a source of potential product failure but also could present safety issues. When contaminants are physically small and difficult to isolate from the product, it is possible to non-destructively characterize the unknown materials in place through the use of FTIR microscopy. FTIR microscopy combines the magnification and images of visual microscopy with the ability to identify unknown materials using infrared spectra. Whether the application involves pharmaceuticals, food, plastics, or electronic components, the first and foremost question to be answered is, “what are the contaminants?” The foreign material needs to be identified so the source of contamination can be determined and future contamination avoided.

FTIR microscopy is a powerful analytical technique used to identify contaminants at specific locations within a sample. By utilizing visual imaging to pinpoint the precise spot of contamination, the infrared spectrum from that targeted area can be collected, allowing for accurate identification of the contaminant. This method is most effective for samples with a limited number of contaminant spots, as it necessitates manual selection and analysis of each location individually. Alternatively, FTIR microscopy can employ mapping to create a comprehensive image of the sample area. In this mapping approach, infrared spectra are systematically collected across a predefined region, generating detailed infrared images that reveal the distribution of various components or contaminants. The mapping technique is especially advantageous for detecting impurities that are difficult to locate visibly; it is also useful for identifying multiple types of contaminants dispersed throughout the sample. Although FTIR imaging offers a more thorough analysis compared to single-point analysis, it also requires additional time. Therefore, the decision to select either single-point analysis or mapping should be guided by the specific requirements of the analysis.

To illustrate the use of FTIR imaging in contaminant analysis, the results of an analysis of several silicon drift detector (SDD) elements are presented here. A silicon drift detector senses X-ray energy as part of an energy dispersive spectroscopy system used in electron microscopy analysis. During analyses performed on an SEM (scanning electron microscope) or TEM (transmission electron microscope), X-rays are generated when the electron beam causes the ejection of an inner orbital electron from the sample and an outer orbital electron drops down to take its place. Each emitted X-ray has a specific energy related to a particular element in the sample; an SDD detects this, and identification of this energy is then used to determine elemental information about the sample.

Contamination of an SDD could occur outside of the SEM or within the SEM. There is a vacuum environment within the SEM, and the surface of the SDD is exposed to this vacuum. This presents multiple potential sources of contamination that include the pumping system, O-rings and other seals, and degassing from samples. Identification of the contaminants is necessary to facilitate tracing the origin of the contaminants and avoiding future contamination.

Experimental

The data presented in this note was collected using a Thermo Scientific™ Nicolet™ iN10 MX Infrared Microscope. Virtually the whole SDD detector surface areas were imaged using a liquid nitrogen cooled linear array detector with a pixel size of 25 microns and 16 scans per spectrum. The spectra were collected in reflection mode off the surface of the detector element.

Results

The visual image of the surface of the SDD detector element is shown in Figure 1. The contamination is readily visible and spreads across the surface. The area imaged, indicated by the red rectangle, is $10,500 \times 5,625 \mu\text{m}^2$. The infrared images shown in Figure 2 (a, b, and c) were generated from different aspects (peak areas and correlation) of the 95,146 spectra that make up the imaging data set and show the spatial distribution of three different types of contaminants. In the infrared images the colors range from blue to red, where the blue represents either no or low intensity or correlation while the red indicates the highest intensity or correlation, with other colors representing values in between these. Since the images are based on spectral features of the various contaminants, they serve as a way to observe the spatial distribution of the contaminants. Also included in Figure 2 are spectra that are representative of the contaminants that give rise to each image.

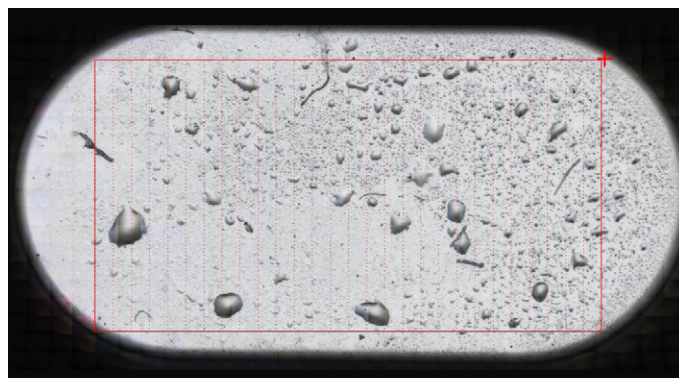


Figure 1. Visual mosaic image of the first contaminated SDD collected with the iN10 MX. The red rectangle indicates the area ($10,500 \mu\text{m} \times 5,625 \mu\text{m}$) designated for FTIR imaging (see Figure 2).

Spectrum 2a is consistent with a long chain hydrocarbon oil such as mineral oil. Mineral oil is used in numerous products and can be used by itself or as a base for blended oils. Spectrum 2b is also likely an oil but has additional components or additives. It is consistent with hydraulic and gear oils where additives are added to reduce wear. This oil looks to have some type of ester additive that is evident by the additional peaks in the spectrum. Another possible source of an ester such as a terephthalate could be from plasticizers found in parts such as O-rings. The third type of contaminant (Spectrum 2c) is consistent with cellulose and can be seen as small fibers and particles. Since the SDD is used in an SEM in a vacuum environment it is possible that oil contamination might have come from the vacuum system, but tracing the contamination back to the source is a subsequent step and will not be addressed here. The cellulose could be from textiles; the oil on the surface might cause cellulose particles to stick to it when otherwise they might not be retained.

The infrared images in Figure 2 provide additional information by showing the distribution of the contaminants across the surface of the SDD. The contaminant shown in Figure 2b is present as discrete particles or droplets, as opposed to the contaminant in Figure 2a which is spread out more evenly across the surface. It is possible to manually measure the size of the particles or droplets, but this becomes tedious if the number of features is large. To facilitate this distribution analysis, it is possible to do an image analysis to obtain size and shape information on all the features. An image analysis of the infrared image shown in Figure 2b found 65 droplets with areas ranging from $3,750$ to $45,1870 \mu\text{m}^2$. If it is assumed the droplets are approximately circular, this would correspond to diameters of 69 to $758 \mu\text{m}$. Figure 3 shows a plot of the size distribution of the droplets found in Figure 2b. The number of cellulose particles in Figure 2c does not require a similarly detailed image analysis, but the image clearly shows some fibers of cellulose along with particles. The fact that some of the cellulose is present as fibers may provide some clues as to the source.

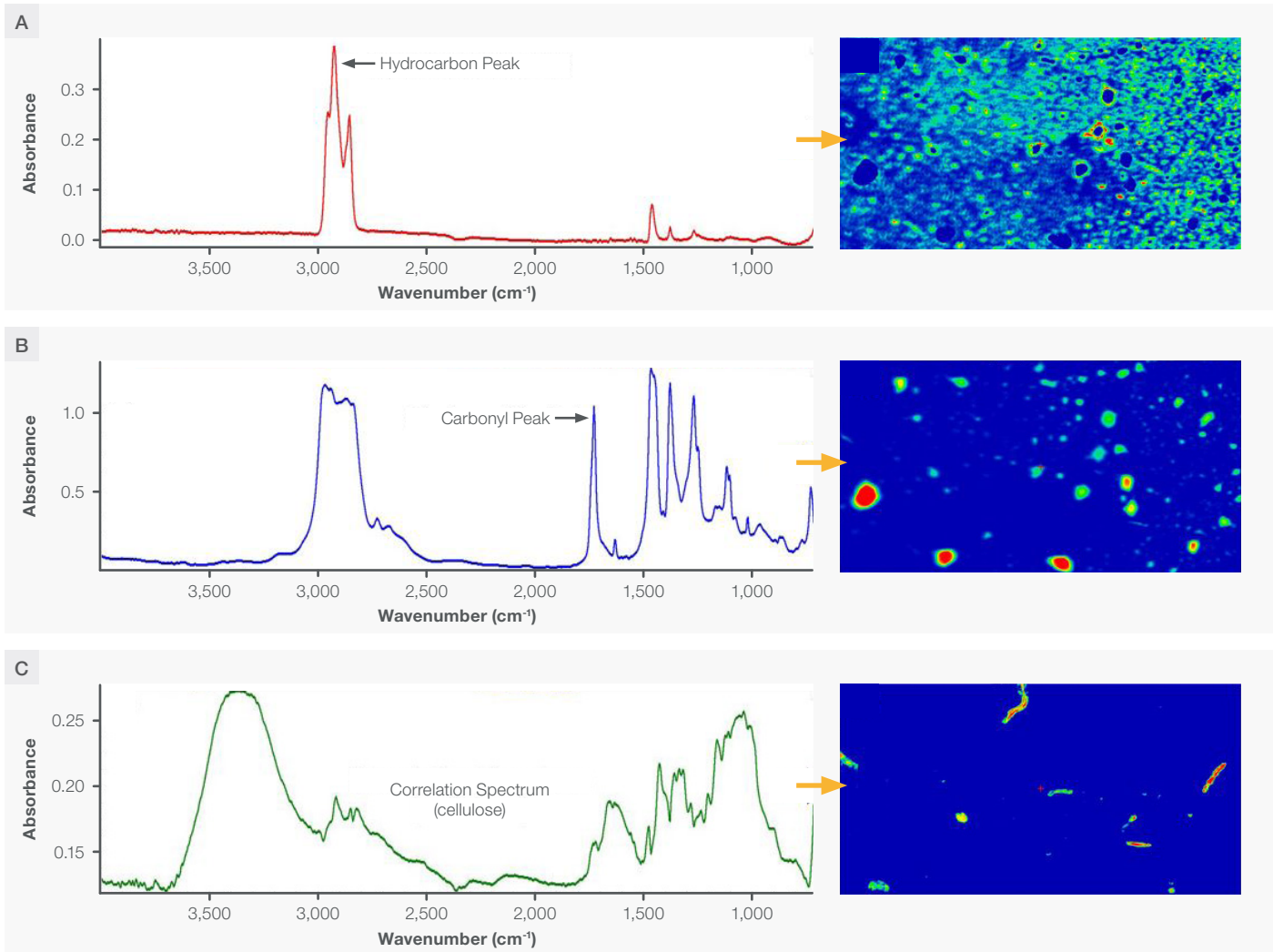


Figure 2. False color infrared images of the area on the first contaminated SDD (see Figure 1). The colors represent peak intensities (A,B) or degree of correlation (C) and range from blue where the values are lowest through green and yellow and finally to red where the values are the highest. (A) An infrared image based on the peak area (2931-2881 cm⁻¹) of the hydrocarbon oil spectrum shown adjacent to the image; (B) An infrared image based on the ester carbonyl peak area (1771-1684 cm⁻¹) shown in the corresponding spectrum; (C) The infrared image based on a correlation to the spectrum of cellulose from the sample shown in the adjoining spectrum.

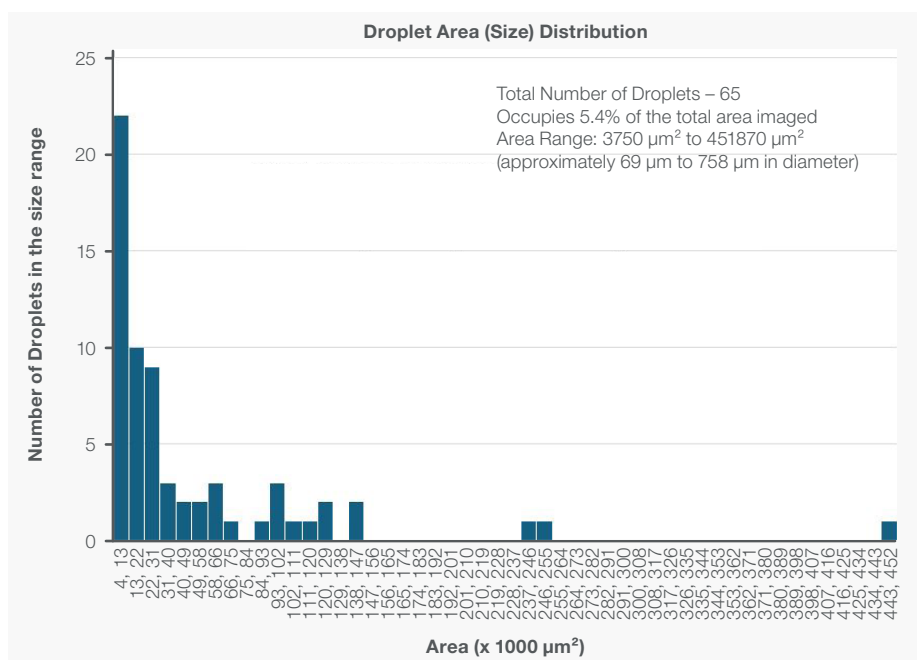


Figure 3. Histogram of the size distribution (areas) of the oil droplets shown in infrared image 2b.

A second example is shown in Figure 4. The visual image shows a more finely dispersed contamination for most of the surface except in the center area of the SDD. FTIR imaging of the area defined by the red rectangle (9,375 x 5,850 μm^2) shows results similar to the previous sample (see Figure 5). It is contaminated by similar materials, but the distribution and relative amounts are different. Most of the well dispersed contamination appears to be mineral oil while there is much less of the ester-containing oil (31 droplets, diameters 41-360 μm , 0.63% of the total area). There are some small (29-114 μm diameter) particles of cellulose but smaller amounts than in the first sample and no clear fibers.

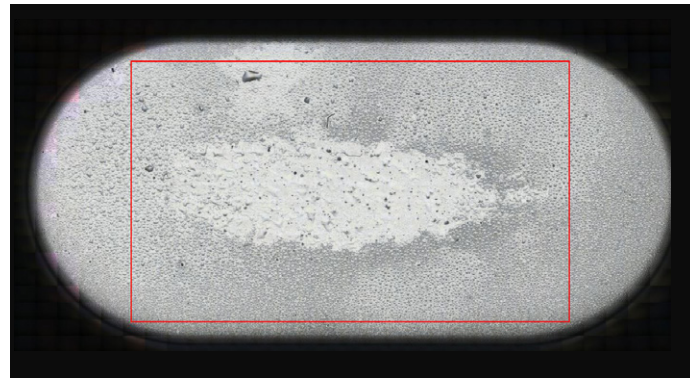


Figure 4. Visual mosaic image of the second contaminated SDD collected with the iN10 MX. The red rectangle indicates the area (9375 x 5850 μm^2) selected for FTIR imaging (see Figure 5).

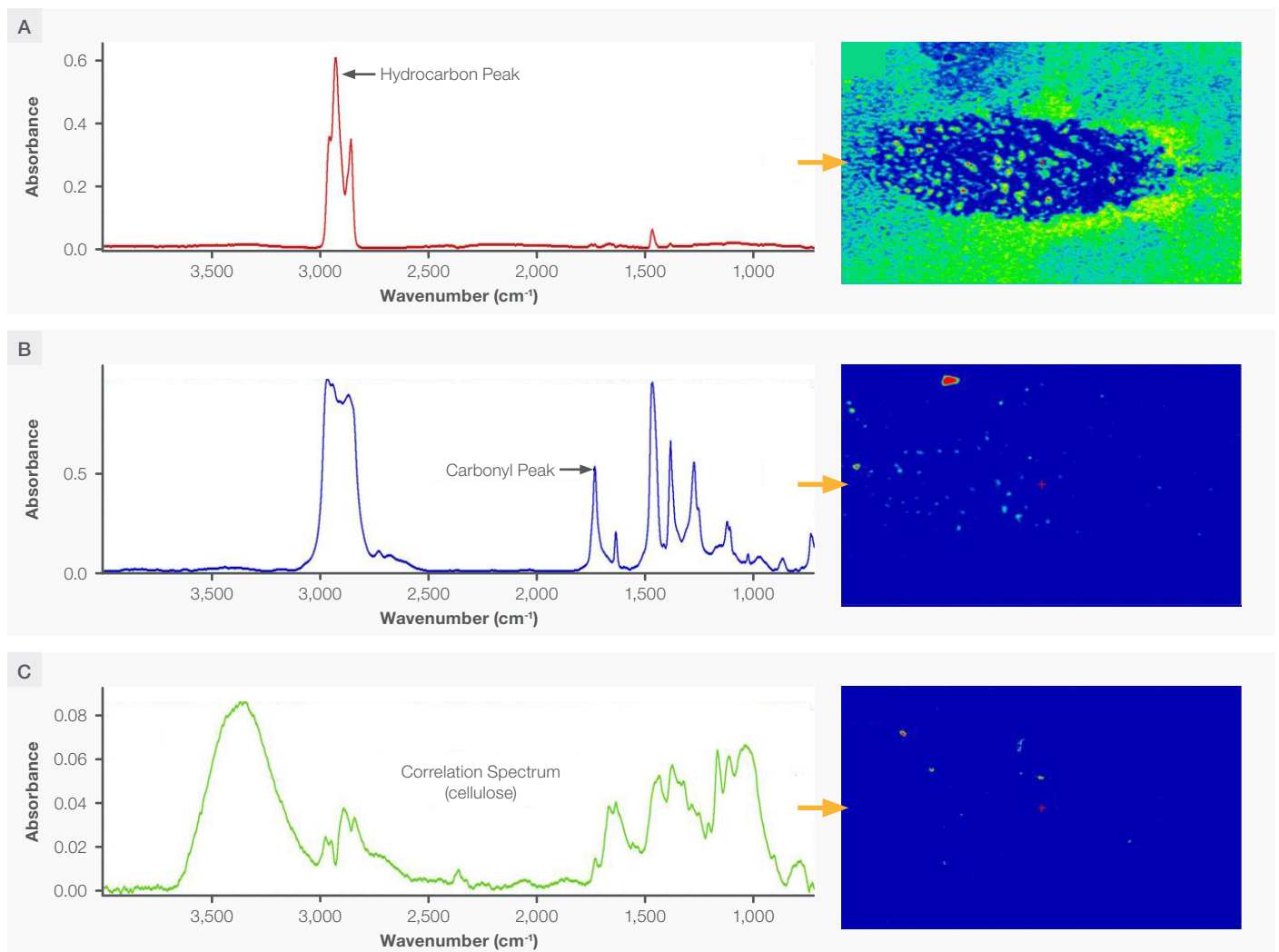


Figure 5. False color infrared images of the area on the second contaminated SDD. The colors represent peak intensities (A,B) or degree of correlation (C) and range from blue where the values are lowest through green and yellow and finally to red where the values are the highest. (A) An infrared image based on the peak area (2931-2881 cm^{-1}) of the hydrocarbon oil spectrum shown adjacent to the image; (B) An infrared image based on the ester carbonyl peak area (1771-1684 cm^{-1}) shown in the corresponding spectrum; (C) The infrared image based on a correlation to the spectrum of cellulose from the sample shown in the adjoining spectrum.

The last example is a reasonably clean SDD (Figure 6) that is shown primarily as a reference. Only a few particles are apparent in the visible image and the infrared images for the most part show very little contamination. Spectrum 7a is consistent with the spectra of proteins but only a few (11) small (30-110 μm diameter) particles are observed. Small particles of proteins from biological sources are common in the environment. Spectrum 7b is consistent with a copolymer containing polyvinyl chloride which might come from something like a plastic wrap. The amount of this contaminant is also very small (9 particles, 32-135 μm in diameter). No evidence for oil contamination was observed at all on this SDD.

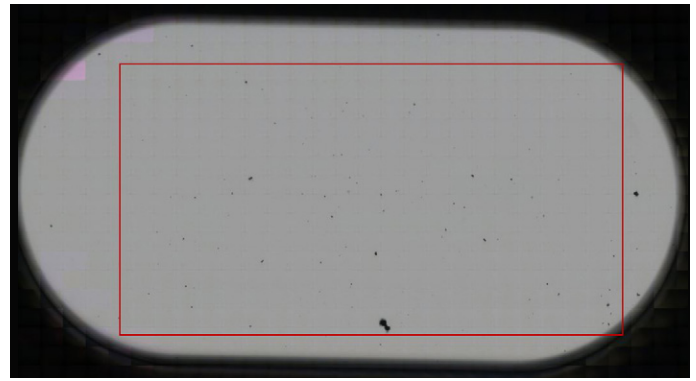


Figure 6. Visual mosaic image of the third (mostly clean) SDD collected with the iN10 MX. The red rectangle indicates the area (10500 x 5250 μm^2) selected for FTIR imaging (see Figure 7).

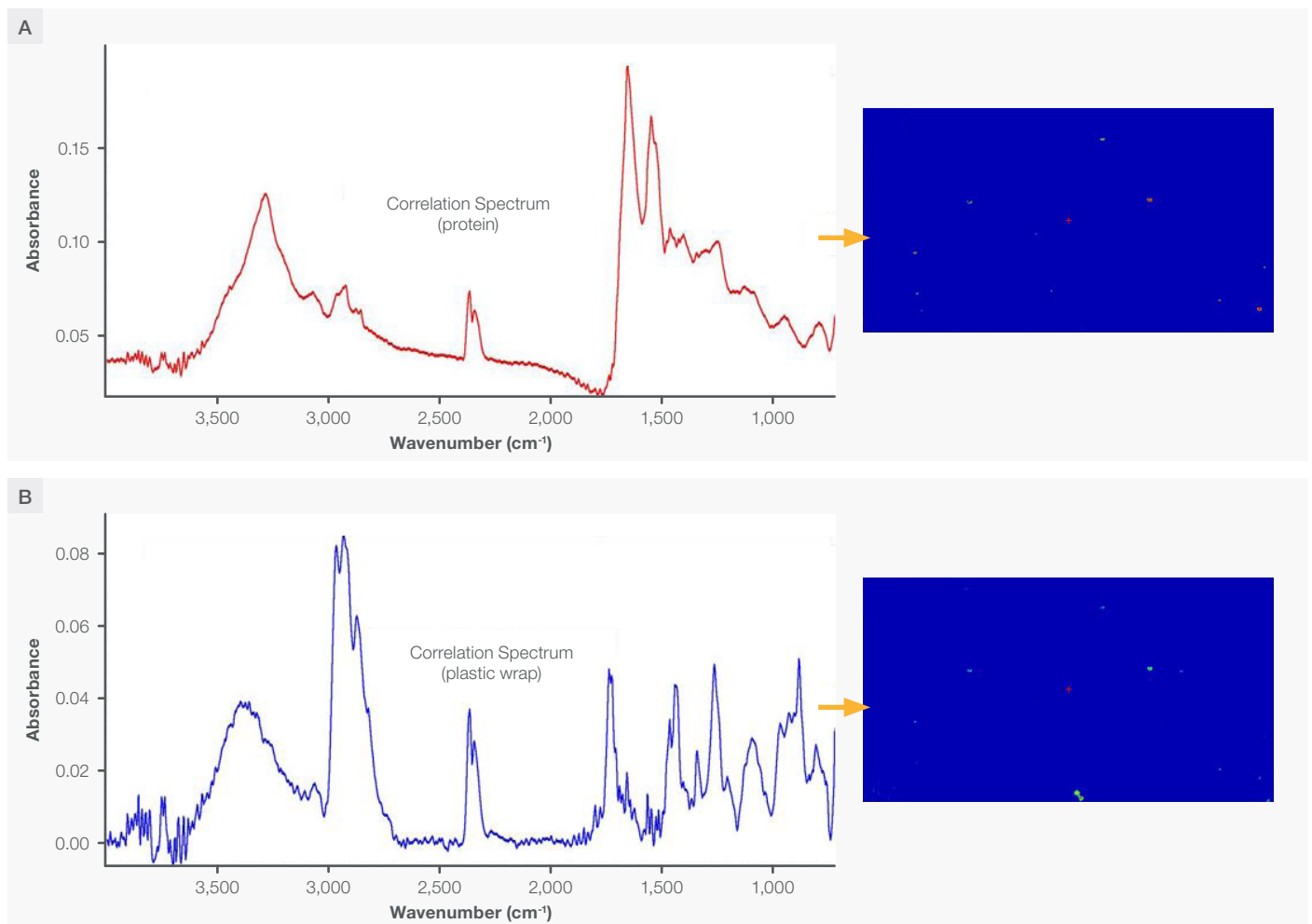


Figure 7. False color infrared images of the area on the third (mostly clean) SDD (see Figure 6). The colors represent the degree of correlation to the associated spectra and range from blue where the values are lowest through green and yellow and finally to red where the values are the highest. (A) An infrared image based on the correlation to the protein spectrum from the sample shown adjacent to the image, (B) An infrared image based on the correlation to the adjoining spectrum from a plastic particle on the sample.

The surfaces of the first two SDDs were quite contaminated. While some of the foreign material such as the cellulose might have been the result of handling and shipping of the devices, the oil contamination certainly was not. The relatively small amount of foreign material on the third SDD would be more representative of what might be expected with exposure to possible environmental contaminants outside of the SEM. While it is possible to have some hydrocarbon contamination in an SEM from things like outgassing of samples and parts or conveyance of contaminants through the vacuum pump, these samples showed the presence of a considerable amount of oil on them. This indicates a significant problem that needs to be rectified.

Conclusion

The examples here illustrate the first step in contamination analysis: Foreign materials need to be identified so they can be traced back to the source. FTIR microscopy might have an additional role later in confirming a link between the source and the observed contamination, but accomplishment of this important first step has been presented here. The first two samples showed considerable contamination but the analysis of the mostly clean SDD demonstrates that is also possible to identify just a few small particulates. The infrared images reveal the spatial distribution of contaminants while also providing size and shape information. This general approach can be applied to other types of samples as well. The iN10 MX Infrared Microscope has good optics that provide an excellent infrared signal, and when combined with the linear array detector it not only allows for efficient imaging of sample areas where contaminants are located and identified, but it is also capable of showing the distribution across the sample.

 Learn more at thermofisher.com/ftir

thermo scientific